ORGANIC CHEMISTRY FRONTIERS

RESEARCH ARTICLE

View Article Online
View Journal | View Issue

Cite this: *Org. Chem. Front.*, 2023, **10**, 1617

Experimental and theoretical studies of the rhodium(I)-catalysed C–H oxidative alkenylation/cyclization of *N*-(2-(methylthio)phenyl) benzamides with maleimides†

Aymen Skhiri, [a] Attila Taborosi, [b,e] Nozomi Ohara,[a] Yusuke Ano, [a] Seiji Mori *[b,d] and Naoto Chatani *[a,c]

The rhodium(I)-catalysed reaction of aromatic amides that contain a 2-(methylthio)aniline directing group with maleimides gives isoindolone spirosuccinimides as products under aerobic, metal oxidant-free, and solvent-free conditions. In sharp contrast to our previous study on the C–H alkylation of aromatic amides in which an 8-aminoquinoline directing group was used, the use of a (2-methylthio)aniline directing group resulted in C–H oxidative alkenylation/cyclization. The maleimide has dual functions, *i.e.*, serving as both a coupling partner and a hydrogen acceptor. Several possible reaction paths were examined by density functional theory (DFT) calculations to clarify the mechanism responsible for the formation of the isoindolone spirosuccinimide products. The results of an in-depth computational study indicate that the reaction proceeds *via* the following main steps: (I) oxidative addition of the *ortho* C–H bond and the migratory insertion of the maleimide, (II) the insertion of a second molecule of maleimide into a Rh–C bond in a rhodacycle with the formation of a C–C bond and subsequent ligand–ligand hydrogen transfer (LLHT), (III) C–N bond formation between the amide and the maleimide, and (IV) PivOH protonation. The use of an energetic span model along with the determination of the kinetic isotopic effect showed that the determining transition state step for the reaction is the oxidative addition/migratory insertion step.

Received 9th January 2023,
Accepted 10th February 2023

DOI: 10.1039/d3qo00023k

rsc.li/frontiers-organic

Introduction

Over the past several decades, the transition-metal-catalysed functionalization of C–H bonds has become one of the most straightforward and ideal strategies for preparing complex molecules from structurally simple compounds.[1] Because of this, the direct functionalization of C–H bonds has now become a reliable tool for the synthesis of a wide variety of natural products, pharmaceuticals, and functional organic materials.[2] Our group previously reported a series of Rh(I)-catalysed C–H alkylation reactions of aromatic amides with various alkenes with the aid of an 8-aminoquinoline directing group.[3,4] When maleimides were used as the alkene coupling partner,[5] C–H alkylation products were selectively formed (Scheme 1a).[4e,m] In addition, it was found that a Ru(II) complex also gave the C–H alkylation product.[4e,6] In sharp contrast, the majority of C–H functionalization reactions of aromatic amides with maleimides reported thus far resulted in the production of isoindolone spirosuccinimide derivatives,[7–15] which are of potential interest in medicinal chemistry.[16] The production of isoindolone spirosuccinimide derivatives was proposed to proceed through an oxidative C–H alkenylation sequence, followed by an intramolecular aza-Michael addition. In 2015, Hirano and Miura reported the copper-mediated reaction of aromatic amides that contain an 8-aminoquinoline directing group with maleimides, leading to the production of isoindolone spirosuccinimides.[8] A similar transformation using $Co(OAc)_2$ as a catalyst was subsequently reported by Jeganmohan.[9] Shi then applied this reaction to enantioselective reactions using Co(II) as a catalyst and spiro phosphoric acid as a chiral ligand.[14] In 2018, Zhai reported Co(II)-catalyzed reactions of aromatic amides using a 2-(1-methylhydrazinyl)pyridine group as the directing group.[11]

[a]*Department of Applied Chemistry, Osaka University, Suita, Osaka 565-0871, Japan. E-mail: chatani@chem.eng.osaka-u.ac.jp*
[b]*Institute of Quantum Beam Science, Ibaraki University, Mito, Ibaraki 310-8512, Japan. E-mail: seiji.mori.compchem@vc.ibaraki.ac.jp*
[c]*Research Center for Environmental Preservation, Osaka University, Suita, Osaka 565-0871, Japan*
[d]*Frontier Research Center for Applied Sciences, Ibaraki University, Tokai, Ibaraki 319-1106, Japan*
[e]*Research Initiative for Supra-Materials, Shinshu University, Nagano, Nagano 380-8553, Japan*

†Electronic supplementary information (ESI) available. CCDC 1966217. For ESI and crystallographic data in CIF or other electronic format see DOI: https://doi.org/10.1039/d3qo00023k

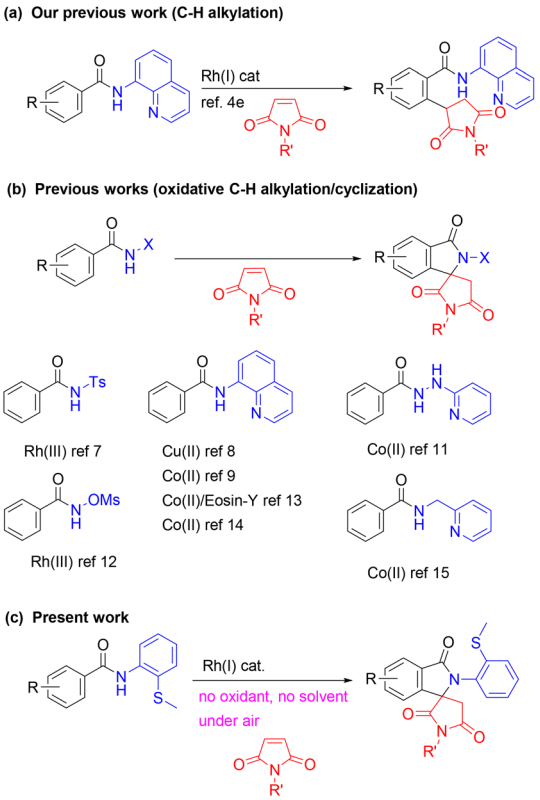

Scheme 1 Previous studies of the Rh(I)-catalyzed reaction of aromatic amides with maleimides and the present work.

Jeganmohan also reported on the Rh(III)-catalyzed synthesis of isoindolone spirosuccinimide derivatives through C–H/N–H/N–O activation using *N*-methoxy benzamides.[12] Ghosh recently reported the room-temperature synthesis of isoindolone spirosuccinimide derivatives from aromatic amides and maleimides using an 8-aminoquinoline directing group in conjunction with a visible-light photocatalyst and a cobalt(II) catalyst.[13] These previously reported reactions required the use of a stoichiometric amount of a Cu salt as a promoter,[8] or an external[7,9,11,14,15] or internal oxidant[12] to regenerate a key catalytic species. We herein report the Rh(I)-catalysed reaction of aromatic amides that contain a (2-methylthio)aniline directing group with maleimides, leading to the production of isoindolone spirosuccinimides. In contrast to previous reports, the present reaction system does not require a metal oxidant and the maleimide group functions as both a coupling partner and a hydrogen acceptor. In addition, the difference in the reaction path between our previous work[4e,m] and this work was evaluated by DFT calculations.

Results and discussion

We began our studies by investigating suitable directing groups for using in reactions of various aromatic amides **1** with *N*-methylmaleimide (**2a**) (Scheme 2). Only an amide containing a (2-methylthio)aniline directing group,[17] as in **1a**, gave **3aa** in 65% yield, but no alkylation products were formed.

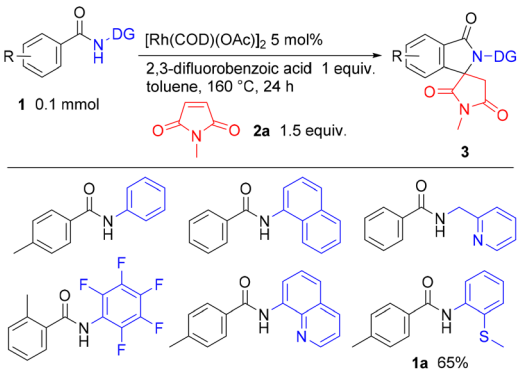

Scheme 2 Screening of directing groups.

We next screened various rhodium catalysts and oxidants in the reaction of **1a** with **2a** (see Tables S1 and S2 in the ESI† for details). Among the rhodium complexes that were examined, $[Rh(COD)Cl]_2$ gave the best results, with **3aa** being produced in 84% NMR yield, along with 12% of the unreacted starting amide **1a** being recovered. Surprisingly, no C–H alkylation product formed in any of these reactions. Among the oxidants examined, MnO_2 gave a higher product yield than other Cu and Ag oxidants (Table S2†). Based on the results obtained in the preliminary screenings, we decided to use $[Rh(COD)Cl]_2$ as the catalyst and MnO_2 as the oxidant. We then continued to optimize the reaction conditions in attempts at increasing the yield of the desired product **3aa** (Table S3†). In initial experiments, we examined the amount of MnO_2 that is used in the reaction. An inverse relationship was found, *i.e.*, the product yields decreased with increasing amounts of MnO_2. In the case of carboxylic acid additives, a higher loading gave higher product yields. Among carboxylic acids that were examined, pivalic acid was found to be the additive of choice and the use of 3 equivalents of **2a** gave the best results. Interestingly, the efficiency of the reaction increased with decreasing amounts of the solvent. We ultimately concluded that the conditions shown in entry 18 in Table S3† were the optimal reaction conditions: **1a** (0.1 mmol), **2a** (0.3 mmol), $[Rh(COD)Cl]_2$ (0.005 mmol), pivalic acid (0.3 mmol), no solvent under an atmosphere of air at 160 °C for 24 h. Under these optimal reaction conditions, **3aa** was obtained in 91% isolated yield.

With the optimized conditions in hand, the scope of maleimides for the reaction was then examined (Scheme 3). The reaction of **1a** with *N*-alkyl maleimides **2a–2d** gave high yields of the corresponding products **3aa–3ad**. The structure of **3aa** was confirmed by an X-ray crystallographic analysis. The reaction of *N*-phenyl maleimide (**2e**) also gave the desired spiro product **3ae** in 65% yield. The reaction of **1a** with **2c** was successfully carried out on a 2-gram scale with only a slightly diminished yield of **3ac**.

We next examined the scope of the reaction with respect to the amide being used (Scheme 4). Halogen atoms, such as Cl, Br, and F were tolerated, with the corresponding halogenated spirosuccinimides **3ba**, **3bd**, **3da**, **3ea**, **3ia**, and **3ja** being pro-

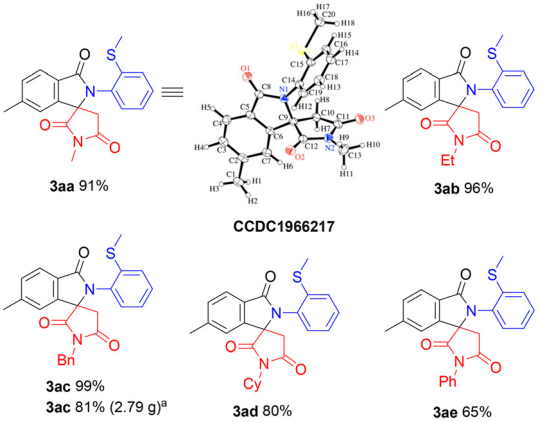

Scheme 3 Screening of maleimide derivatives. Reaction conditions: **1a** (0.1 mmol), **2** (0.3 mmol), $[Rh(COD)Cl]_2$ (0.005 mmol), PivOH (0.3 mmol) under air at 160 °C for 24 h. [a] The reaction was carried out on a 2 g scale (7.77 mmol of **1a**).

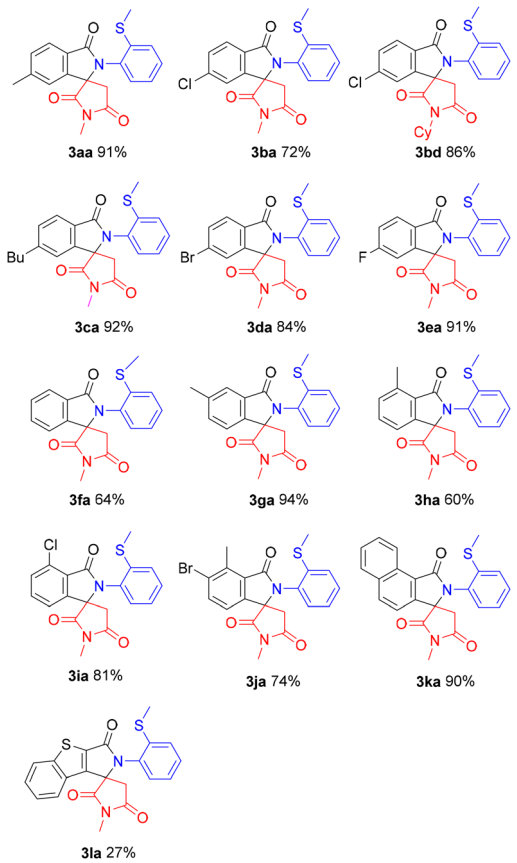

Scheme 4 Substrate scope. Reaction conditions: **1** (0.1 mmol), **2a** (0.3 mmol), $[Rh(COD)Cl]_2$ (0.05 mmol), PivOH (0.3 mmol) under air at 160 °C for 24 h.

duced, which could be further elaborated to produce a variety of useful compounds by cross-coupling reactions. In the reaction of the *meta*-methyl substrate **1g**, only the less hindered C–H bond was selectively functionalized to give **3ga** in 94% yield. The reaction was also applicable to naphthalene-1-carboxamide (**1k**) and benzothiophene-1-carboxamide (**1l**), affording the corresponding spiro products.

Deuterium labelling experiments using **1f-d_5** were carried out to gain insights into the reaction mechanism (Scheme 5a). The reaction of **1f-d_5** with **2c** gave **3fc-d_4** in 42% yield, with 58% of the starting amide being recovered. A significant amount of H/D exchange was observed at the *ortho*-position in both the recovered amide (0.52D) and the product (0.70D). Deuterium incorporation was also observed in the recovered maleimide **2c**. In contrast, in the reaction of **1a** with the deuterated maleimide **2c-d_2** (Scheme 5b), negligible D-incorporation was observed in both the product and in the recovered amide. H/D exchange also took place at the *ortho*-position when **1a** was treated with CD_3CO_2D instead of PivOH in the absence of a maleimide (Scheme 5c). We next examined the difference in reactivity between **1f** and **1f-d_5** in parallel experiments (Scheme 5d). A KIE value k_H/k_D of 2.5 was obtained, suggesting that the cleavage of the C–H bond is the rate-determining step.

It was found that a maleimide functions as both a coupling partner and a hydrogen acceptor in this reaction. In fact, the formation of a succinimide was observed, but the mass balance was not high (Scheme 6).

A proposed mechanism for the reaction is shown in Scheme 7. The sulfur atom in **1f** coordinates to Rh(I)X and a subsequent ligand exchange gives **A** along with the generation of HX. The oxidative addition of the *ortho* C–H bond to the Rh

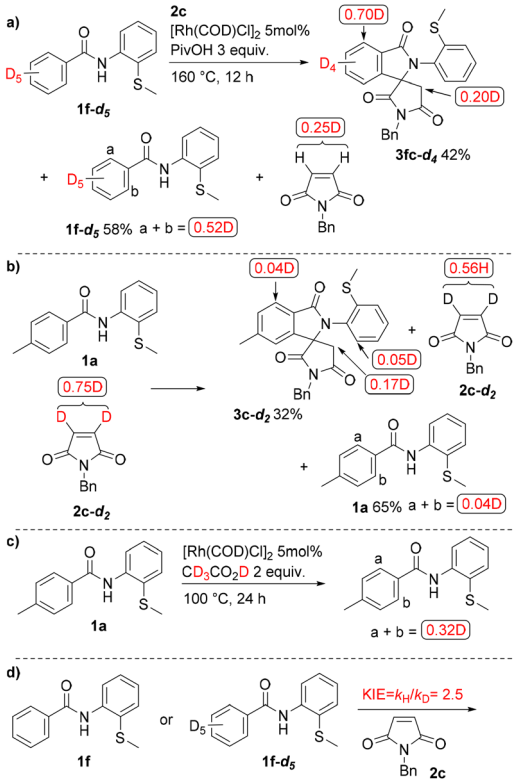

Scheme 5 Deuterium labelling studies.

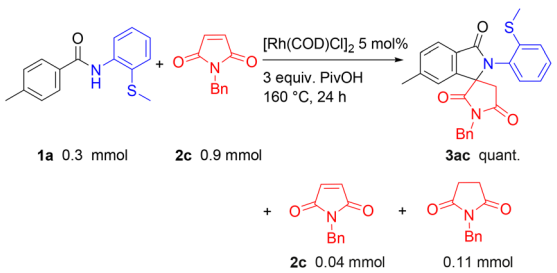

Scheme 6 Maleimide as a hydrogen acceptor.

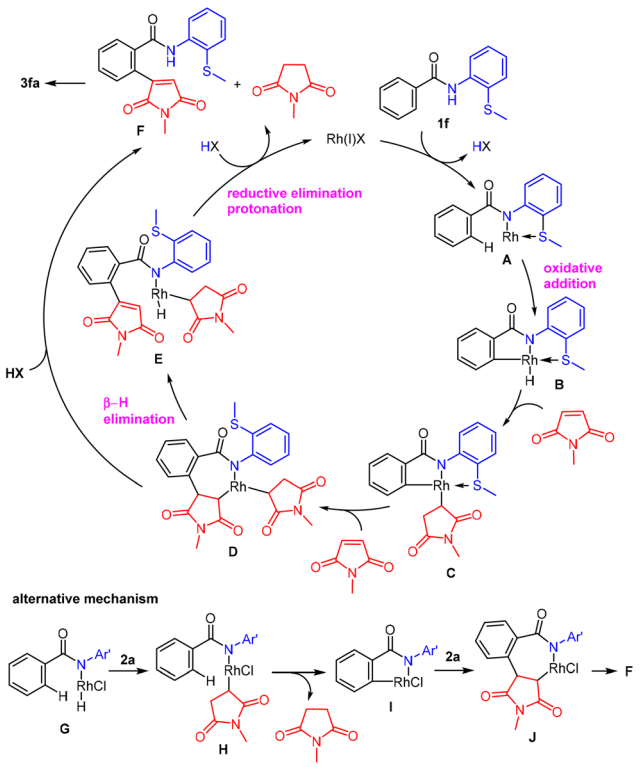

Scheme 7 A proposed mechanism.

center in **A** gives a five-membered rhodacycle **B.** The migratory insertion of a maleimide into an H–Rh bond in **B** generates **C**, which is followed by the insertion of a second molecule of a maleimide into the C–Rh bond in **C** to give **D**, along with dissociation of a sulfur atom. β-Hydride elimination from **D** gives **E**, which undergoes reductive elimination followed by protonation to give **F** with the concomitant generation of a succinimide and the regeneration of the Rh(I) species. Compound **F** then undergoes intramolecular aza-Michael-type addition to give spiro-succinimide **3fa.** The results shown in Scheme 5a–c indicate that the steps involving the cleavage of the *ortho* C–H bond and the insertion of a maleimide are both reversible. Alternatively, one step directly from complex **D** gives **F** and a succinimide could occur without passing through complex **E.**

A possible alternative mechanism (Scheme 7, bottom), which could involve the initial coordination of a sulfur atom in **1f** to Rh(I)X followed by the oxidative addition of a N–H bond to a Rh(I) center giving hydride Rh(III) complex **G,** cannot be excluded.[18] The insertion of a maleimide in the resulting H–Rh bond in **G** gives complex **H** and the subsequent activation of the *ortho* C–H bond *via* σ-bond metathesis gives a five-membered rhodacycle **I** with the generation of *N*-methylsuccinimide. The insertion of a second maleimide molecule in a C–Rh bond in **I** gives **J**, which affords **F** through β-hydride elimination.

To clarify the reaction mechanism, we carried out DFT calculations for the reaction mechanisms at the M06[19]/def2-TZVP[20]/SMD[21]+W[22,23]+cc level (Computational details can be found in the ESI†). The reaction is initiated by the coordination of Rh^{I}(COD)(OPiv) to *N*-(2-(methylthio)phenyl)benzamide (Fig. 1, **INT-0**) to form the Rh(I) complex (**INT-1**). The S atom coordinates to the Rh center (Rh–S = 2.40 Å), while one of the O atoms of pivalate interacts with the H of the amide group *via* hydrogen bonding, and the bond between the other O atom and Rh(I) (Rh–O = 2.08 Å) is maintained. Catalyst coordination is followed by the deprotonation of N–H (**TS-1**) with an activation energy of 120 kJ mol^{-1} and the dissociation of pivalic acid (PivOH) from the Rh(I) complex (**INT-2**).

Two possible reaction paths were considered for the C–H activation steps after N–H deprotonation, namely oxidative addition/migratory insertion (OA/MI) and ligand–ligand hydrogen transfer (LLHT). The C–H bond activation step at the LLHT path occurred after the maleimide coordinated to the complex (**INT-3B**) and through an LLHT between the phenyl group and maleimide with an activation energy of 172 kJ mol^{-1} (**TS-2B**). The bonding between the S atom of the methylsulfanyl group and Rh (Rh–S = 2.50 Å) in intermediate **INT-4B** with a sp^3-C_α–Rh is maintained and the oxidation state of Rh changes from (I) to (III). A possible alternative path for the C–H activation through oxidative addition/migratory insertion in the absence of maleimide (**TS-2A**) with 191 kJ mol^{-1} activation energy was also considered. In this scenario, Rh(I) is bonded to hydrogen from the phenyl group of the aromatic amide (**INT-3A**), and the oxidation state of Rh changes from (I) to (III) as evidenced by oxidative addition. After the oxidative addition, the maleimide coordinates to the Rh(III)-complex (**INT-4A**), and the S atom simultaneously dissociates from Rh(III). The migratory insertion (**TS-3A**) is the next transition step with an activation energy of 39 kJ mol^{-1} and the formation of the **INT-5A** complex, which is very similar to that of **INT-4B**, except that the S atom of the methylsulfanyl group dissociates.

The formation of a C–C bond between the second maleimide and the phenyl group of an aromatic amide with the insertion of the second maleimide and LLHT steps were considered. However, these steps were evaluated with and without the formation of bonds between COD (cyclooctadiene) and Rh(III). The second maleimide coordinates with the Rh(III) complex after migratory insertion or ligand–ligand hydrogen transfer. This could occur either in the presence or absence of COD as a ligand substituent between the maleimide and COD. If the bonding between COD and Rh(III) is maintained, the S atom would remain dissociated from Rh(III) (**INT-6C**), but, if

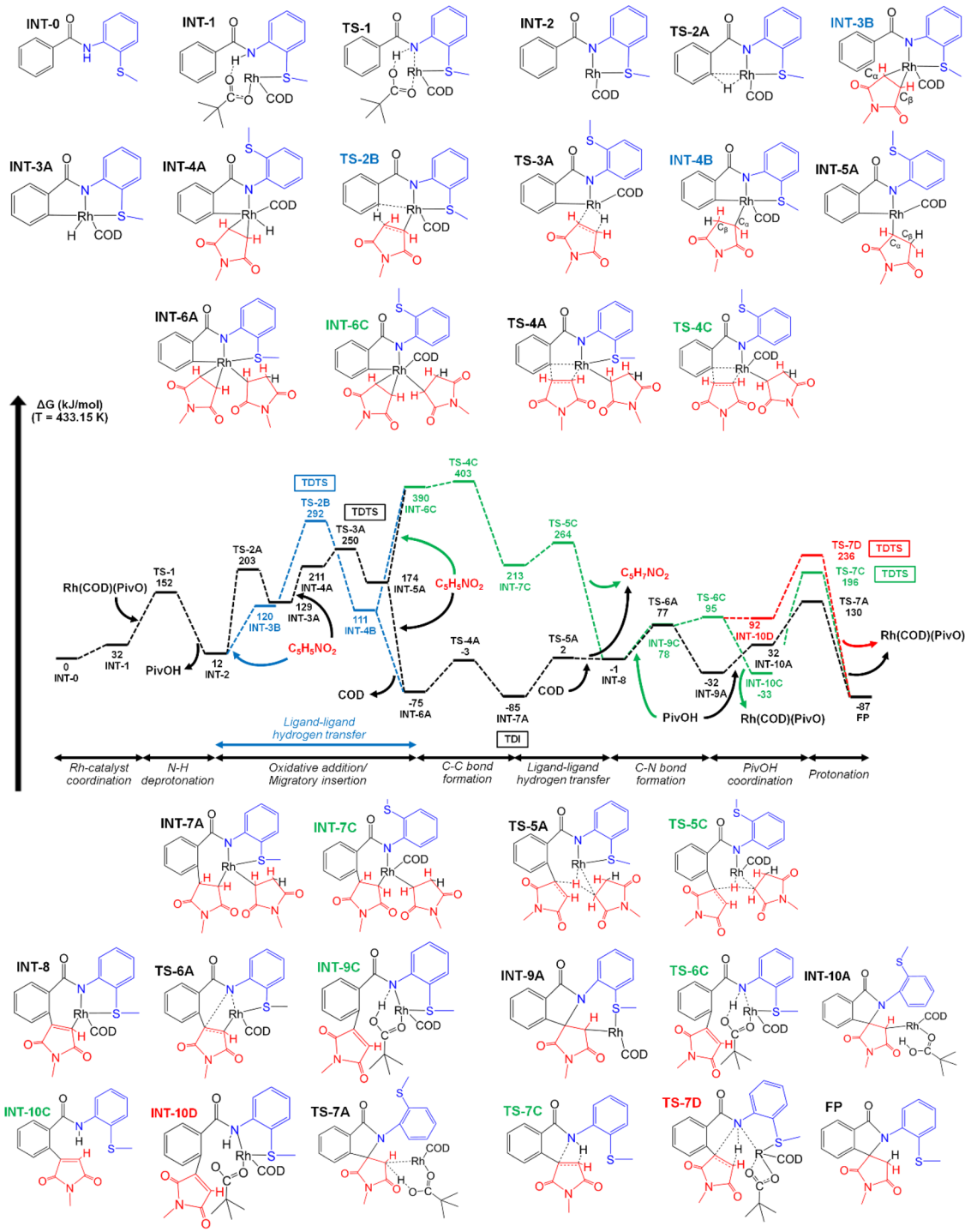

Fig. 1 The Gibbs free energy profile (kJ mol^{-1}, T = 433.15 K) of rhodium(I)-catalyzed alkylation of the C–H bond in a (2-methylthio)aniline directing group with maleimide computed at the M06/def2-TZVP/SMD+W+cc level.

COD is dissociated from the Rh(III)-complex, the S atom would form a bond with Rh(III) and one of the O atoms of the maleimide would also coordinate to the transition metal. Through the **TS-4A**/**TS-4C** transition state steps, C–C bond formation occurs between the maleimide and phenyl group of the aromatic amide with 72 kJ mol^{-1} (**TS-4A**, absence of COD) and 13 kJ mol^{-1} (**TS-4C**, presence of COD), respectively. The C–C bond formation step is followed by LLHT, whereas the Rh-bonded maleimide dissociates from the complex, as it becomes protonated, while COD re-coordinates to the Rh(I)-complex between **TS-5A** and **INT-8**. Thus, the reaction is proposed to proceed through an anomalous type of LLHT process

involving Rh catalysis which is rare compared to other catalysis such as that of Ni,[24–27] Mn,[28] Mo,[29] or Pd.[30]

Several alternative paths were also considered for the formation of the final products (isoindolone spirosuccinimides) from *N*-(2-(methylthio)phenyl)benzamides. Thus, three alternative paths were considered and examined after the re-coordination of COD to the Rh complex (**INT-8**). Two possible steps were investigated, one of which involves C–N bond formation through **TS-6A** and the other involves the re-coordination of PivOH to the Rh complex (**INT-9C**). The re-coordination of PivOH is followed by the protonation of the amide group (**TS-6C**), and C–N bond formation occurs through the C/D paths. In these cases, bond formation was investigated for both the presence and absence of a Rh-complex (**TS-7C**/**TS-7D**). Overall, we can conclude that the presence of a Rh–COD catalyst without coordinated PivOH is the most preferable for the C–N bond formation (**TS-6A**, 78 kJ mol^{-1}). The presence of both the catalyst and re-coordinated PivOH greatly increases the activation energy for the C–N bond formation (**TS-7C**, 229 kJ mol^{-1}), while the absence of both of them slightly decreases this activation energy (**TS-7D**, 144 kJ mol^{-1}).

The C–N bond formation (**TS-6A**) step was followed by the re-coordination of PivOH (**INT-10A**) and the protonation of C_β of the maleimide (**TS-7A**) with an activation energy of 98 kJ mol^{-1}.

Utilization of the energetic span model[31] showed a different TOF-determined intermediate (TDI) and a TOF-determining transition state (TDTS) for the different scenarios. There are two possible TDIs; the preference for which depends on whether C–C bond formation occurs with (**INT-6A** → **TS-5A** path) or without (**INT-6C** → **TS-5C** path) the presence of COD. Therefore, if the **INT-6C** alternative path is considered, then **INT-2** is the TDI, but, if the **INT-6A** path is considered, then **INT-7A** is the TDI. Since the **INT-6C** path is not preferable over the **INT-6A** path, we did not consider it further. In the first part of the reaction, where C–H bond activation paths were considered (OA/MI and LLHT), the calculated TDTS was the **TS-2B** step for LLHT and **TS-3A** for OA/MI. The calculated energetic span for the TDTS **TS-2B** was 207 kJ mol^{-1} ($G_{\mathbf{TS\text{-}2B}} - G_{\mathbf{INT\text{-}7A}}$), while that for TDTS **TS-3A** was 165 kJ mol^{-1} ($G_{\mathbf{TS\text{-}3A}} - G_{\mathbf{INT\text{-}7A}}$). Therefore, the OA/MI path is preferred over the LLHT path. In the end, if we consider the **TS-6A** → **TS-7A** path, **TS-3A** is the TDTS; however, for the C and D paths **TS-7C** and **TS-7D** are the TDTSs of the entire reaction, which is not consistent with the experimental observations.

An energy decomposition analysis[32] (EDA) was also performed on the key intermediate and transition state structures (OA/MI, LLHT and C–C bond formation) of the reaction paths to clarify the differences. These structures were divided into two fragments, *i.e.*, (2-methylthio)aniline aromatic amide [A] and Rh–COD or Rh–COD–mal complexes [B] (Fig. S1†). More details regarding the determination and explanation of the different parts (ΔE_{int}, ΔE_{orb}, ΔE_{steric} and ΔE_{disp}) of energy decomposition analysis can be found in the ESI.† The calculated interaction energies (Table S8†) show a reasonable similarity with the determined Gibbs free energies of the reaction paths. In the OA/MI and LLHT section of the reaction paths, **INT-2** have the lowest (ΔE_{int} = −1228 kJ mol^{-1}) interaction energy, where the orbital term (ΔE_{orb} = −1473 kJ mol^{-1}) greatly stabilizes the complex. In contrast, the steric term does not cause significant destabilization (ΔE_{steric} = 245 kJ mol^{-1}). Furthermore, the calculated dispersion energy was the lowest compared to that of the other structures; thus non-covalent interactions are also less significant in **INT-2**. The OA/MI paths for **TS-2A** (ΔE_{int} = −719 kJ mol^{-1}) and **INT-3A** (ΔE_{int} = −778 kJ mol^{-1}) already showed a larger interaction energy compared to those for **INT-2** and **INT-3B** (but smaller compared to that for **TS-3B**), due the formation of a bond between H and Rh. The orbital term decreases, while the steric term increases as the sign of destabilization effect on **TS-2A** and **INT-3A** complexes. However, non-covalent interactions and the dispersion energy do not significantly increase compared to **INT-2**. Furthermore, **TS-2B** of the LLHT path showed a higher interaction energy (ΔE_{int} = −633 kJ mol^{-1}) compared to **TS-2A** of the OA/MI path (ΔE_{int} = −719 kJ mol^{-1}) suggesting that the LLHT path is less preferred not just energetically, but is also the less stable structure because of a significant steric term (ΔE_{steric} = 886 kJ mol^{-1}) destabilization of **TS-2B**. Interestingly **INT-4A** (ΔE_{int} = −597 kJ mol^{-1}) and **TS-3A** (ΔE_{int} = −605 kJ mol^{-1}) showed a slightly higher interaction energy compared to **TS-2B**; however the Gibbs free energies of these structures were slightly lower. Overall, the coordination of the maleimide greatly destabilizes the Rh-complex, thus also increasing the steric term and dispersion energy. During the C–C bond formation, the absence of COD (**INT-6A**, **TS-4A**) was preferable over the presence of COD (**INT-6C**, **TS-4C**). The difference in the interaction energy can also be discovered, as the absence of COD gave a stable Rh-complex compared to the presence of COD.

Intermediates **TS-2A**, **TS-2B**, **TS-3A**, **TS-7C** and **TS-7D** were considered for the theoretical determination of the kinetic isotopic effect (KIE) to further clarify the alternative reaction paths and as a comparison with the experimentally determined values. The value for the **TS-2A**, **TS-2B** and **TS-3A** steps were 2.89, 3.39, and 2.95, quite similar to the experimental value of 2.5. The KIE values for **TS-7C** and **TS-7D** (1.02 and 0.97) were much lower compared to the experimentally determined values. If we consider the tunnelling correction, the theoretical values of **TS-2A** and **TS-3A** slightly increase (3.36 and 3.12), while that of **TS-2B** drastically increased (9.31).

Conclusions

We report some solvent-free, Rh(I)-catalyzed reactions of aromatic amides with maleimides with the aid of a (2-methylthio) aniline directing group, leading to the production of isoindolone spirosuccinimide derivatives under aerobic conditions, without the need for toxic metallic oxidants or expensive additives. Maleimides have dual roles in the reaction; in which they function as both a coupling partner and hydrogen acceptor. In sharp contrast to the findings reported in our previous

study,[4e] the use of a (2-methylthio)aniline directing group did not result in the formation of C–H alkylation products. DFT computations predicted that the reaction proceeds *via* an oxidative addition/migratory insertion (OA/MI) step rather than ligand–ligand hydrogen transfer after N–H deprotonation by a pivalate ion bonded to the Rh center. The OA/MI step is the TOF-determining transition state (TDTS) of the catalytic reaction. PivOH participates in the last step after C–N bond formation, leading to the formation of an isoindolone spirosuccinimide.

Author contributions

Experimental work and data analysis were performed by A. S. and N. O.; computational work was performed by A. T., Y. A., and S. M.; N. C. supervised the project; A. T., S. M., and N. C. wrote the manuscript. The manuscript was written with the discussion and approval of all authors.

Conflicts of interest

There are no conflicts to declare.

Acknowledgements

This work was supported by a Grant in Aid for Specially Promoted Research by MEXT (no. 17H06091 to N. C.) and a Grant-in-Aid for Scientific Research (C) by JSPS (no. JP21K05016 to S. M.). The generous allotment of computation time in the Research Center for Computation Science, the National Institutes of Natural Sciences, Okazaki, Japan is gratefully acknowledged (project: 21-IMS-C046 and 22-IMS-C046).

Notes and references

1 For recent reviews on C–H functionalization, see: (*a*) T. Yoshino and S. Matsunaga, Cp*Co^{III}-Catalyzed C-H Functionalization and Asymmetric Reactions Using External Chiral Sources, *Synlett*, 2019, 1384; (*b*) S. M. Khake and N. Chatani, Chelation-Assisted Nickel-Catalyzed C-H Functionalizations, *Trends Chem.*, 2019, **1**, 524; (*c*) P. Gandeepan, T. Müller, D. Zell, G. Cera, S. Warratz and L. Ackermann, 3d Transition Metals for C-H Activation, *Chem. Rev.*, 2019, **119**, 2192; (*d*) C. He, W. Whitehurst and M. J. Gaunt, Palladium-Catalyzed C(sp^3)-H Bond Functionalization of Aliphatic Amines, *Chem*, 2019, **5**, 1031; (*e*) J. Diesel and N. Cramer, Generation of Heteroatom Stereocenters by Enantioselective C-H Functionalization, *ACS Catal.*, 2019, **9**, 9164; (*f*) S. Rej and N. Chatani, Rhodium-Catalyzed C(sp^2)- or C(sp^3)-H Bond Functionalization Assisted by Removable Directing Groups, *Angew. Chem., Int. Ed.*, 2019, **58**, 8304; (*g*) A. Dey, S. K. Sinha, T. K. Achar and D. Maiti, Accessing Remote meta- and para-C(sp^2)-H Bonds with Covalently Attached Directing Groups, *Angew. Chem., Int. Ed.*, 2019, **58**, 10820; (*h*) J. Loup, U. Dhawa, F. Pesciaioli, J. Wencel-Delord and L. Ackermann, Enantioselective C-H Activation with Earth-Abundant 3d Transition Metals, *Angew. Chem., Int. Ed.*, 2019, **58**, 12803; (*i*) S. Rej, Y. Ano and N. Chatani, Bidentate Directing Groups: An Efficient Tool in C-H Bond Functionalization Chemistry for the Expedient Construction of C-C Bonds, *Chem. Rev.*, 2020, **120**, 1788; (*j*) Q. Zhao, G. Meng, S. P. Nolan and M. Szostak, N-Heterocyclic Carbene Complexes in C-H Activation Reactions, *Chem. Rev.*, 2020, **120**, 1981; (*k*) Q. Shao, K. Wu, Z. Zhuang, S. Qian and J.-Q. Yu, From Pd(OAc)$_2$ to Chiral Catalysts: The Discovery and Development of Bifunctional Mono-N-Protected Amino Acid Ligands for Diverse C-H Functionalization Reactions, *Acc. Chem. Res.*, 2020, **53**, 833; (*l*) A. Trowbridge, S. M. Walton and M. J. Gaunt, New Strategies for the Transition-Metal Catalyzed Synthesis of Aliphatic Amines, *Chem. Rev.*, 2020, **120**, 2613; (*m*) T. Yoshino, S. Satake and S. Matsunaga, Frontispiece: Diverse Approaches for Enantioselective C-H Functionalization Reactions Using Group 9 Cp^{x}M^{III} Catalysts, *Chem. – Eur. J.*, 2020, **26**, 7346; (*n*) J. Jeon, C. Lee, I. Park and S. Hong, Regio- and Stereoselective Functionalization Enabled by Bidentate Directing Groups, *Chem. Rec.*, 2021, **21**, 3613; (*o*) K. Korvorapun, R. C. Korkit, C. Ramesh, T. Rogge and L. Ackermann, Remote C-H Functionalizations by Ruthenium Catalysis, *Synthesis*, 2021, 2911; (*p*) E. L. Lucas, N. Y. S. Lam, Z. Zhuang, H. S. S. Chan, D. A. Strassfeld and J.-Q. Yu, Palladium-Catalyzed Enantioselective β-C(sp^3)-H Activation Reactions of Aliphatic Acids: A Retrosynthetic Surrogate for Enolate Alkylation and Conjugate Addition, *Acc. Chem. Res.*, 2022, **55**, 537; (*q*) S. K. Sinha, S. Guin, S. Maiti, J. P. Biswas, S. Porey and D. Maiti, Toolbox for Distal C-H Bond Functionalizations in Organic Molecules, *Chem. Rev.*, 2022, **122**, 5682; (*r*) R. S. Thombal, P. Y. M. Rubio, D. Lee, D. Maiti and Y. R. Lee, Modern Palladium-Catalyzed Transformations Involving C-H Activation and Subsequent Annulation, *ACS Catal.*, 2022, **12**, 5217.

2 For recent reviews on applications of C–H functionalizations in complex natural product synthesis or material synthesis, see: (*a*) T. Brandhofer and O. G. Mancheno, Site-Selective C-H Bond Activation/Functionalization of Alpha-Amino Acids and Peptide-Like Derivatives, *Eur. J. Org. Chem.*, 2018, 6050; (*b*) D. J. Abrams, P. A. Provencher and E. J. Sorensen, Recent applications of C-H functionalization in complex natural product synthesis, *Chem. Soc. Rev.*, 2018, **47**, 8925; (*c*) I. A. Stepek and K. Itami, Recent Advances in C-H Activation for the Synthesis of π-Extended Materials, *ACS Mater. Lett.*, 2020, **2**, 951–974; (*d*) Y. Zhang and M. Szostak, Synthesis of Natural Products by C-H Functionalization of Heterocycless, *Chem. – Eur. J.*, 2022, **28**, e202104278.

3 N. Chatani, The Use of a Rhodium Catalyst/8-Aminoquinoline Directing Group in the C-H Alkylation of

Aromatic Amides with Alkenes: Possible Generation of a Carbene Intermediate from an Alkene, *Bull. Chem. Soc. Jpn.*, 2018, **91**, 211.

4 For our papers on the Rh(I)-catalyzed C–H functionalization, see: (*a*) K. Shibata and N. Chatani, Rhodium-Catalyzed Alkylation of C-H Bonds in Aromatic Amides with α,β-Unsaturated Esters, *Org. Lett.*, 2014, **16**, 5148; (*b*) K. Shibata, T. Yamaguchi and N. Chatani, Rhodium-Catalyzed Alkylation of C-H Bonds in Aromatic Amides with Styrenes via Bidentate–Chelation Assistance, *Org. Lett.*, 2015, **17**, 3584; (*c*) K. Shibata and N. Chatani, Rhodium-catalyzed regioselective addition of the ortho C-H bond in aromatic amides to the C-C double bond in α,β-unsaturated γ-lactones and dihydrofurans, *Chem. Sci.*, 2016, **7**, 240; (*d*) K. Shibata, S. Natsui and N. Chatani, Rhodium-Catalyzed Alkenylation of C-H Bonds in Aromatic Amides with Alkynes, *Org. Lett.*, 2017, **19**, 2234; (*e*) Q. He, T. Yamaguchi and N. Chatani, Rh(I)-Catalyzed Alkylation of ortho-C-H Bonds in Aromatic Amides with Maleimides, *Org. Lett.*, 2017, **19**, 4544; (*f*) K. Shibata, S. Natsui, M. Tobisu, Y. Fukumoto and N. Chatani, An unusual endo-selective C-H hydroarylationof norbornene by the Rh(I)-catalyzed reactionof benzamides, *Nat. Commun.*, 2017, **8**, 1448; (*g*) Q. He and N. Chatani, A Synthesis of 3,4-Dihydroisoquinolin-1(2H)-one via the Rhodium-Catalyzed Alkylation of Aromatic Amides with N-Vinylphthalimide, *J. Org. Chem.*, 2018, **83**, 13587; (*h*) S. Rej and N. Chatani, Rhodium(I)-Catalyzed C8-Alkylation of 1-Naphthylamide Derivatives with Alkenes through a Bidentate Picolinamide Chelation System, *ACS Catal.*, 2018, **8**, 6699; (*i*) T. Yamaguchi, S. Natsui, K. Shibata, K. Yamazaki, S. Rej, Y. Ano and N. Chatani, Rhodium-Catalyzed Alkylation of C-H Bonds in Aromatic Amides with Non-activated 1-Alkenes: The Possible Generation of Carbene Intermediates from Alkenes, *Chem. – Eur. J.*, 2019, **25**, 6915; (*j*) S. Rej and N. Chatani, Rhodium(I)-catalyzed mono-selective C-H alkylation of benzenesulfonamides with terminal alkenes, *Chem. Commun.*, 2019, **55**, 10503; (*k*) S. Rej and N. Chatani, Rh(II)-catalyzed branch-selective C-H alkylation of aryl sulfonamides with vinylsilanes, *Chem. Sci.*, 2020, **11**, 389; (*l*) N. Ohara, S. Rej and N. Chatani, Rh(I)-catalyzed Addition of the ortho C-H Bond in Aryl Sulfonamides to Maleimides, *Chem. Lett.*, 2020, **49**, 1053; (*m*) A. Taborosi, Q. He, Y. Ano, N. Chatani and S. Mori, Reaction Path Determination of Rhodium(I)-Catalyzed C-H Alkylation of N-8-Aminoquinolinyl Aromatic Amides with Maleimides, *J. Org. Chem.*, 2022, **87**, 737.

5 For recent reviews on C–H functionalization using maleimides as coupling partners, see: (*a*) R. Manoharan and M. Jaganmohan, Alkylation, Annulation, and Alkenylation of Organic Molecules with Maleimides by Transition-Metal-Catalyzed C-H Bond Activation, *Asian J. Org. Chem.*, 2019, **8**, 1949; (*b*) S.-L. Liu, Y. Shi, C. Xue, L. Zhang, L. Zhou and M.-P. Song, Maleimides in Directing-Group-Controlled Transition-Metal-Catalyzed Selective C-H Alkylation, *Eur. J. Org. Chem.*, 2021, 5862.

6 P. Keshri, K. R. Bettadapur, V. Lanke and K. R. Prabhu, Ru (II)-Catalyzed C-H Activation: Amide-Directed 1,4-Addition of the Ortho C-H Bond to Maleimides, *J. Org. Chem.*, 2016, **81**, 6056.

7 (*a*) C. Zhu and J. R. Falck, Rhodium catalyzed C-H olefination of N-benzoylsulfonamides with internal alkenes, *Chem. Commun.*, 2012, **48**, 1674; (*b*) C. Zhu and J. R. Falck, Rhodium catalyzed synthesis of isoindolinones via C-H activation of N-benzoylsulfonamides, *Tetrahedron*, 2012, **68**, 9192.

8 W. Miura, K. Hirano and M. Miura, Copper-Mediated Oxidative Coupling of Benzamides with Maleimides via Directed C-H Cleavage, *Org. Lett.*, 2015, **17**, 4034.

9 R. Manoharan and M. Jeganmohan, Cobalt-Catalyzed Oxidative Cyclization of Benzamides with Maleimides: Synthesis of Isoindolone Spirosuccinimides, *Org. Lett.*, 2017, **19**, 5884.

10 N. Lv, Y. Liu, C. Xiong, Z. Liu and Y. Zhang, Cobalt-Catalyzed Oxidant-Free Spirocycle Synthesis by Liberation of Hydrogen, *Org. Lett.*, 2017, **19**, 4640.

11 H. Zhao, X. Shao, T. Wang, S. Zhai, S. Qiu, C. Tao, H. Wang and H. Zhai, A 2-(1-methylhydrazinyl)pyridine-directed C-H functionalization/spirocyclization cascade: facile access to spirosuccinimide derivatives, *Chem. Commun.*, 2018, **54**, 4927.

12 B. Ramesh, M. Tamizmani and M. Jeganmohan, Rhodium (III)-Catalyzed Redox-Neutral 1,1-Cyclization of N-Methoxy Benzamides with Maleimides via C-H/N-H/N-O Activation: Detailed Mechanistic Investigation, *J. Org. Chem.*, 2019, **84**, 4058.

13 C. Sen, B. Sarvaiya, S. Sarkar and S. C. Ghosh, Room-Temperature Synthesis of Isoindolone Spirosuccinimides: Merger of Visible-Light Photocatalysis and Cobalt-Catalyzed C-H Activation, *J. Org. Chem.*, 2020, **85**, 15287.

14 W.-K. Yuan and B.-F. Shi, Synthesis of Chiral Spirolactams via Sequential C-H Olefination/Asymmetric [4+1] Spirocyclization under a Simple Co^{II}/Chiral Spiro Phosphoric Acid Binary System, *Angew. Chem., Int. Ed.*, 2021, **60**, 23187.

15 M. Xu, Y. Yu, Y. Wang, Y. Mu, H. Xie and Y. Li, Cobalt-catalyzed C-bond activation of N-carbamoyl indoles or benzamides with maleimides: Synthesis of imidazo[1,5-a]indole- or isoindolone-incorporated spirosuccinimides, *Tetrahedron Lett.*, 2021, **70**, 152872.

16 (*a*) J. Wrobel, A. Dietrich, S. A. Woolson, J. Millen, M. McCaleb, M. C. Harrison, T. C. Hohman, J. Sredy and D. Sullivan, Novel Spirosuccinimides with Incorporated Isoindolone and Benzisothiazole 1,1-Dioxide Moieties as Aldose Reductase Inhibitors and Antihyperglycemic Agents, *J. Med. Chem.*, 1992, **35**, 4613; (*b*) H. M. Botero Cid, C. Tränkle, K. Baumann, R. Pick, E. Mies-Klomfass, E. Kostenis, K. Mohr and U. Holzgrabe, Structure-Activity Relationships in a Series of Bisquaternary Bisphthalimidine Derivatives Modulating the Muscarinic M2-Receptor Allosterically, *J. Med. Chem.*, 2000, **43**, 2155; (*c*) M. Shi, J. Lu and M. S. Shoichet, Organic nanoscale drug carriers coupled with ligands for targeted drug deliv-

ery in cancer, *J. Mater. Chem.*, 2009, **19**, 5485; (*d*) G. S. Singh and Z. Y. Desta, Isatins As Privileged Molecules in Design and Synthesis of Spiro-Fused Cyclic Frameworks, *Chem. Rev.*, 2012, **112**, 6104; (*e*) K. Hu, D. Patnaik, T. L. Collier, K. N. Lee, H. Gao, M. R. Swoyer, B. H. Rotstein, H. S. Krishnan, S. H. Liang, J. Wang, Z. Yan, J. M. Hooker, N. Vasdev, S. J. Haggarty and M. Y. Ngai, Development of [^{18}F]Maleimide-Based Glycogen Synthase Kinase-3β Ligands for Positron Emission Tomography Imaging, *ACS Med. Chem. Lett.*, 2017, **8**, 287; (*f*) S. Chortani, M. Othman, A. M. Lawson, A. Romdhane, H. B. Jannet, M. Knorr, L. Briegar, C. Strohmann and A. Daich, Aza-heterocyclic frameworks through intramolecular π-system trapping of spiro-N-acyliminiums generated from isoindolinone, *New J. Chem.*, 2021, **45**, 2393.

17 For the first use of a (2-methylthio)aniline directing group in C–H functionalization, see: D. Shabashov and O. Dauglulis, Auxiliary-assisted palladium-catalyzed arylation and alkylation of sp^2 and sp^3 carbon-hydrogen bonds, *J. Am. Chem. Soc.*, 2010, **132**, 3965.

18 (*a*) S. A. Macgregor, Theoretical Study of the Oxidative Addition of Ammonia to Various Unsaturated Low-Valent Transition Metal Species, *Organometallics*, 2001, **20**, 1860; (*b*) J. Zhao, A. S. Goldman and J. F. Hartwig, Oxidative addition of ammonia to form a stable monomeric amido hydride complex, *Science*, 2005, **307**, 1080.

19 Y. Zhao and D. G. Truhlar, The M06 suite of density functionals for main group thermochemistry, thermochemical kinetics, noncovalent interactions, excited states, and transition elements: two new functionals and systematic testing of four M06-class functionals and 12 other functionals, *Theor. Chem. Acc.*, 2008, **120**, 215.

20 F. Weigend and R. Ahlrichs, Balanced basis sets of split valence, triple zeta valence and quadruple zeta valence quality for H to Rn: Design and assessment of accuracy, *Phys. Chem. Chem. Phys.*, 2005, **7**, 3297.

21 A. V. Marenich, C. J. Cramer and D. G. Truhlar, Universal solvation model based on solute electron density and on a continuum model of the solvent defined by the bulk dielectric constant and atomic surface tensions, *J. Phys. Chem. B*, 2009, **113**, 6378.

22 M. Mammen, E. I. Shakhnovich, J. M. Deutch and G. M. Whitesides, Estimating the Entropic Cost of Self-Assembly of Multiparticle Hydrogen-Bonded Aggregates Based on the Cyanuric Acid·Melamine Lattice, *J. Org. Chem.*, 1998, **63**, 3821.

23 M. C. Schwarzer, R. Konno, T. Hojo, A. Ohtsuki, K. Nakamura, A. Yasutome, H. Takahashi, T. Shimasaki, M. Tobisu, N. Chatani and S. Mori, Combined Theoretical and Experimental Studies of Nickel-Catalyzed Cross-Coupling of Methoxyarenes with Arylboronic Esters via C-O Bond Cleavage, *J. Am. Chem. Soc.*, 2017, **139**, 10347.

24 J. Guihaume, S. Halbert, O. Eisenstein and R. N. Perutz, Hydrofluoroarylation of Alkynes with Ni Catalysts. C-H Activation via Ligand-to-Ligand Hydrogen Transfer, an Alternative to Oxidative Addition, *Organometallics*, 2012, **31**, 1300.

25 S. Nakanowatari, T. Muller, J. C. A. Oliveira and L. Ackermann, Bifurcated Nickel-Catalyzed Functionalizations: Heteroarene C-H Activation with Allenes, *Angew. Chem., Int. Ed.*, 2017, **56**, 15891.

26 A. Obata, A. Sasagawa, K. Yamazaki, Y. Ano and N. Chatani, Nickel-catalyzed oxidative C-H/N-H annulation of N-heteroaromatic compounds with alkynes, *Chem. Sci.*, 2019, **10**, 3242.

27 J. Ma, X. Zhao, D. Zhang and S. Shi, Enantio- and Regioselective Ni-Catalyzed para-C-H Alkylation of Pyridines with Styrenes via Intermolecular Hydroarylation, *J. Am. Chem. Soc.*, 2022, **144**, 13643.

28 L. Massignan, C. Zhu, J. C. A. Oliveira, A. Salame and L. Ackermann, Manganaelectro-Catalyzed Azine C-H Arylations and C-H Alkylations by Assistance of Weakly Coordinating Amides, *ACS Catal.*, 2021, **11**, 11639.

29 D. Zhai, S. Xie, Y. Xia, H. Fang and Z. Shi, Silylamido supported dinitrogen heterobimetallic complexes: syntheses and their catalytic ability, *Natl. Sci. Rev.*, 2021, **8**, nwaa290.

30 A. Y. Jiu, H. S. Slocumb, C. S. Yeung, X. Yang and V. M. Dong, Enantioselective Addition of Pyrazoles to Dienes, *Angew. Chem., Int. Ed.*, 2021, **60**, 19660.

31 S. Kozuch and S. Shaik, How to Conceptualize Catalytic Cycles? The Energetic Span Model, *Acc. Chem. Res.*, 2011, **44**, 101.

32 K. Kitaura and K. Morokuma, A New Energy Decomposition Scheme for Molecular Interactions within the Hartree-Fock Approximation, *Int. J. Quantum Chem.*, 1976, **10**, 325.